APPLICATION OF TOUGH TO HYDROLOGIC PROBLEMS RELATED TO THE UNSATURATED ZONE SITE INVESTIGATION AT YUCCA MOUNTAIN, NEVADA

by Edward M. Kwicklis[1], Richard W. Healy[1], G.S. Bodvarsson[2], and Ning Lu[3]

[1]U.S. Geological Survey
[2]Lawrence Berkeley Laboratory
[3]Foothills Engineering/U.S. Geological Survey

ABSTRACT

To date, TOUGH and TOUGH2 have been the principal codes used by the U.S. Geological Survey in their investigation of the hydrology of the unsaturated zone at Yucca Mountain. As illustrated by the range of particular studies to which they have been applied, these codes have proven very versatile and robust, and, when necessary, adaptable for applications not originally envisioned during their development.

Examples of some applications of the TOUGH and TOUGH2 codes to flow and transport problems related to the Yucca Mountain site investigation are presented, and the slight modifications made to the codes to implement them are discussed. These examples include: (1) The use of TOUGH in a simple fracture network model, with a discussion of an approach to calculate directional relative permeabilities at computational cells located at fracture intersections. These simulations illustrated that, under unsaturated conditions, the locations of dominant pathways for flow through fracture networks are sensitive to imposed boundary conditions; (2) The application of TOUGH to investigate the possible hydrothermal effects of waste-generated heat at Yucca Mountain using a dual-porosity, dual-permeability treatment to better characterize fracture-matrix interactions. Associated modifications to TOUGH for this application included implementation of a lookup table that can express relative permeabilities parallel and transverse to the fracture plane independently. These simulations supported the continued use of an effective media approach in analyses of the hydrologic effects of waste-generated heat; and (3) An investigation of flow and tracer movement beneath a wash at Yucca Mountain in which a particle tracker was used as a post-processor. As part of this study, TOUGH2 was modified to calculate and output the x-,y- and z-components of fluid fluxes and pore velocities as input into the particle tracker. This study suggested that contrasts in hydrologic properties of a layered sequence of tuffs overlying the potential repository site will result in the formation of capillary barriers that locally promote considerable lateral flow, thereby significantly decreasing the magnitude of fluxes from peak values at the ground surface and delaying the arrival of surface-derived moisture at the potential repository horizon.

INTRODUCTION

Yucca Mountain, Nevada, is being investigated as a potential location for a high-level nuclear waste repository. If the site is found suitable, the repository would be located in the unsaturated zone, approximately 250-350m below ground surface, depending on local topography, and 225m above the regional water table. The hydrogeologic environment in which the waste would be placed consists primarily of ash flow and ash-fall tuffs, which have been welded and fractured to varying degrees. In general, the more densely welded tuffs possess lower porosity and primary permeability than the nonwelded or moderately welded tuffs, but are more intensely fractured. The secondary permeability of densely welded tuffs may be six orders of magnitude or more greater than their primary permeability, and several orders of magnitude larger than the primary permeability of the less welded tuffs. As with other arid zone sites where annual precipitation is much less than potential evapotranspiration, the areally-averaged annual flux is believed to be a small fraction of annual precipitation, although net infiltration may be locally large following rainstorms or snowmelt, particulary when infiltration occurs in fractures and can move rapidly away from the ground surface where it might otherwise be removed by evapotranspiration. Because the areally-averaged flux is believed to be small and fractures are probably drained most of the time, the movement of water as vapor is potentially an important component of the overall moisture balance, especially following waste emplacement when a large volume of in situ pore water is likely to be vaporized by waste-generated heat.

The geometric flexibility offered by TOUGH and TOUGH2 has permitted their application to hydrologic problems involving fracture networks, and to mulitphase problems that require consideration of dual-porosity, dual-permeability effects. Their numerical robustness has also allowed their use in numerical investigations of the dynamics of water movment in layered, variably fractured tuff sequences subjected to abrupt changes in boundary conditions.. These applications and the modifications to the TOUGH and TOUGH2 codes that allowed their implementation are described below.

APPLICATIONS

Water Movement in a Variably Saturated Fracture Network

Interest in the mechanisms of water movement in thick, fractured unsaturated zones has occurred only relatively recently, primarily as a result of the possibility of nuclear waste isolation in such environments. Therefore, understanding of the hydrologic behavior of variably saturated fractured rock is not as fully developed as for other hydrogeologic environments. To gain insight into the possible behavior of variably-saturated fractured rock , a numerical study was conducted of water movement through a simple fracture network using TOUGH. Of particular interest was the potential for water flow through the network to become concentrated along specific pathways, and the conditions under which flow behavior was similar to, or deviated strongly from, behavior believed typical of porous media. The intent was that the insight gained would result in better strategies for physically testing or monitoring such media..

A TOUGH compatible integrated finite difference mesh was created for a simple fracture network using FMMG (Okusu et al., 1989), and eliminating the matrix elements, which were assumed impermeable. The network included two fracture sets: a subvertical set containing five fractures and a subhorizontal set containing four fractures. Three sets of simulations were conducted, including: (1) a "mixed" network with subvertical and subhorizontal fractures having average physical apertures of 125 and 25μm, respectively; (2) a geometrically similar network in which all fractures had physical apertures of 125μm; and (3) a network in which fractures had physical apertures of 25μm. The lengths and locations of the fractures were arbitrary and are not

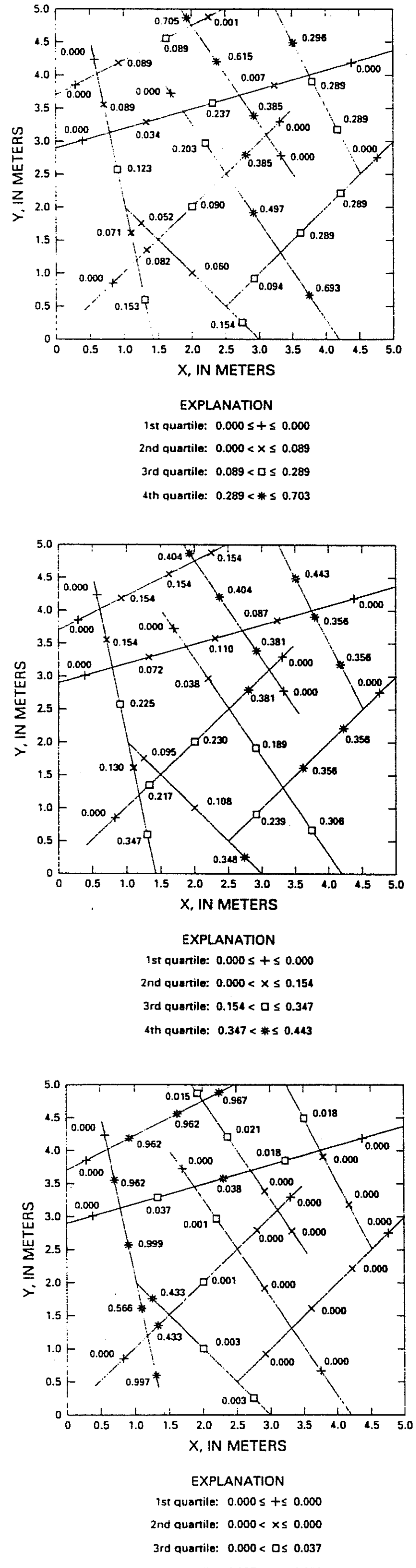

Figure 1. Distribution of fractional flux in the "mixed" network for prescribed boundary pressure heads of (a) 0.0m (b) -0.10m, and (c) -0.25m.

intended to reflect any specific geologic environment. The fracture apertures were within the range of values reported for Yucca Mountain. Unsaturated properties , including effective permeability to water and saturation as functions of pressure head, were determined by a separate numerical model VSFRAC (Kwicklis and Healy, 1993) that considered aperture variability within individual fractures having the cited mean apertures. Average unsaturated hydrologic properties for 10 stochastic realizations of each fracture size were fit with functional forms for ease of incorporation into TOUGH. Water flow under the influence of gravity was simulated for each of the three networks for prescribed upper and lower boundary pressure heads ranging from 0 to -0.25m, in increments of 0.05m.

In performing these simulations, the critical modeling issue was the manner in which the relative permeabilities were determined at cells representing fracture intersections. Directional relative permeabilities were assumed for these cells, with relative permeabilities at each interface calculated on the basis of the capillary pressure of the cell and on the properties assigned to the adjacent fracture segment. A small subroutine was added that expressed relative permeability as a function of capillary pressure. Upstream weighting was used for numerical stability. For numerical stability, it was also necessary that each fracture element along the inflow or outflow boundaries was assigned its own boundary element.

For each boundary condition, the steady-state distributions of water flow and pressure heads were recorded, along with variability in flow and pressure head within the network. Figure 1 shows how the principal flowpaths through the "mixed" network change as a function of the boundary pressure heads. Listed adjacent to each fracture element in Figure 1 is the fractional flux, which is defined as the liquid water flux passing through that element divided by the total flux carried by the network. From these results it can be observed that both the location of the dominant pathways and the variability in normalized flux change with relatively small changes in boundary pressure. The variability in normalized flux (figure 2) reflects the degree to which the flux is either concentrated along specific paths or spread among many pathways in the network. The constant, but nonzero, standard deviations shown in figure 2 for the uniform 25 and 125 µm fracture networks reflect the variability in flux caused by differences in orientation of the elements with respect to gravity. Similar analyses were done for pressure heads within the network. Plots of the variability in flux and pressure

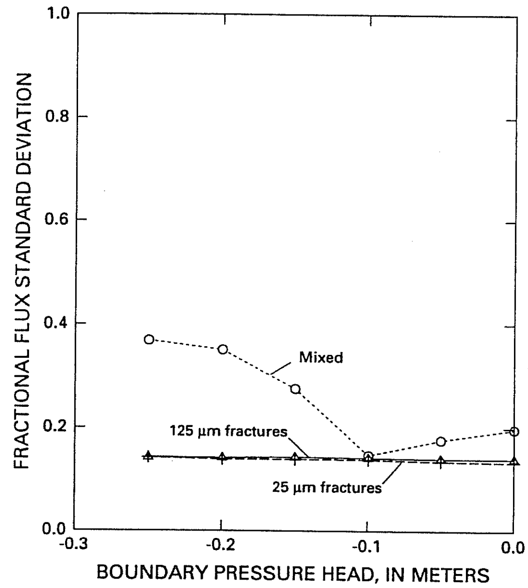

Figure 2. Standard deviation of fractional flux as a function of boundary pressure head for the three fracture networks.

head as a function of boundary pressure head implied that the network behaved more like porous media for some pressure heads, but less so at others.

These results also implied that the locations of dominant flow paths through the fracture network within the unsaturated zone at Yucca Mountain might be quite dynamic and depend on climate-induced changes in boundary conditions at the ground surface. Therefore, observations of the present-day distribution of seeps in tunnels may bear an uncertain relation to the future distribution of seeps.

Dual Porosity - Dual Permeability Simulation of the Hydrologic Effects of Waste-Generated Heat.

With notable exceptions (Pruess et al., 1990a,b), numerical simulations of repository dry-out due to thermal loads generated by radioactive decay of nuclear waste have typically assumed that the use of the equivalent continuum model (ECM) results in negligible error. The ECM assumes that when the temperature at a given location in space has been raised above the boiling point, water at that location can immediately move as vapor within drained portions of the fracture network. The time required for water to move from the central parts of each matrix block to the fracture face (where it is vaporized) is not considered by the ECM. Hence, the extent of the dry-out zone coincides closely with the boiling front (e.g. Buscheck and Nitao, 1993), even when matrix blocks are very large, matrix permeability is very low, and thermal loads and conductivity are very large. Intuitively, one would expect that where matrix block sizes are large, or when matrix permeability is small (due to natural variability or desaturation), the assumption of instantaneous transfer of liquid to the fracture face would be increasingly in error, especially at high thermal loads.. In these cases, both the rate of dry-out and the rate of condensate generation (and, hence, of reflux) would be overestimated by the ECM. This overestimation, if it occurs, may be important because previous studies employing the ECM have concluded that the refluxing of condensate would overwhelm the natural recharge, even for pluvial conditions. The purpose of this study was to compare rates of dry-out and condensate generation predicted from two different models: the equivalent continuum model (ECM) and a true double porosity approach.

The study employs a highly simplified stratigraphy consisting of a single unit with matrix properties thought to be representative of the densely welded Topopah Spring Member. The simplied stratigraphy is justified because the concern here is principally with differences that result from the modeling approach employed, and not in predicting the actual response of Yucca Mountain to thermal loading. The simplified stratigraphy permits these differences to be seen more clearly. Boundary conditions imposed were gas pressure=86,000 Pa, temperature=13 °C, and liquid flux=0.0 at the ground surface, and gas pressure=91,822 Pa, temperature=31 °C, and liquid saturation=1.0 at the water table. These boundary conditions resulted in essentially static equilibrium conditions for both the liquid and gas phases. Simulations employing these boundary conditions were run to long times to establish the initial conditions for the thermal loading calculations.

Hydrologic properties for the ECM model were derived by assuming there are 3 orthogonal fracture sets with 1-m spacing, resulting in matrix blocks that are 1-m^3. Each fracture set was assumed to consist exclusively of fractures with average physical apertures of 25 microns. Moisture characteristic and effective permeability curves for single fractures having average physical apertures of 25 microns were estimated using a numerical model (VSFRAC) which considers aperture variability at the pore-scale. Calculated results that were averages of 10 different realizations of the aperture field were smoothed and extrapolated by fitting closed-form functions. ECM properties were entered in tabular form into TOUGH as a function of gas saturation.

The double-porosity calculations employed the Multiple Interacting Continuum (MINC) approach of Pruess and Narasimhan (1985). Most applications of the MINC method do not allow for block-to-block flow within the matrix continuum. However, it was clearly necessary to consider this process to allow for the possiblity that some or even most of the condensate might reflux back toward the repository through the matrix. Furthermore, the calculations of Buscheck and Nitao (1993) indicated that heat flow was dominated by conduction through the rock matrix, rather than by convection through the fracture system. Therefore, for each fracture continuum cell, the associated lumped matrix block that resulted from application of the MINC approach was connected to similar blocks centered on cells above and below it. Similarly nested shells of these lumped matrix blocks were connected across areas that were determined from the intercell area of the fracture continuum, and the fractional volume of the lumped matrix blocks contained by those shells. By connecting similarly located shells of adjacent matrix blocks in this manner, identical darcy fluxes and head changes within all shells of a given matrix block could, theoretically, be obtained for one-dimensional flow in the absence of interaction with the fracture continuum.

Wet and dry thermal conductivity of the matrix blocks were the same as for the ECM continuum. "Effective" fractures in the fracture continuum were defined as including matrix extending to 0.5 mm from the center plane through the 25 micron fractures. The inclusion of a small amount of matrix into the fracture continuum results in new effective continuum hydraulic conductivity and capillary pressure curves. Similarly, the thermal conductivity and heat capacity of the fracture continuum were calculated as weighted fractions of the analogous matrix quantities. Almost all the thermal conductivity and heat capacity are associated with the matrix continuum, as one would expect given its larger cross-sectional area and volume. The inclusion of some small amount of matrix material in the fracture continuum was done to facilitate the numerical computations by providing additional heat capacity and fluid storage, controlling temperature and saturation changes and thereby permitting larger time steps to be taken than would otherwise be possible (Pruess et al., 1990a,b). Although the small addition of matrix may have dampened the response of the fractures to flow to a small degree, over 99% of the rock mass remained in the matrix continuum, free to

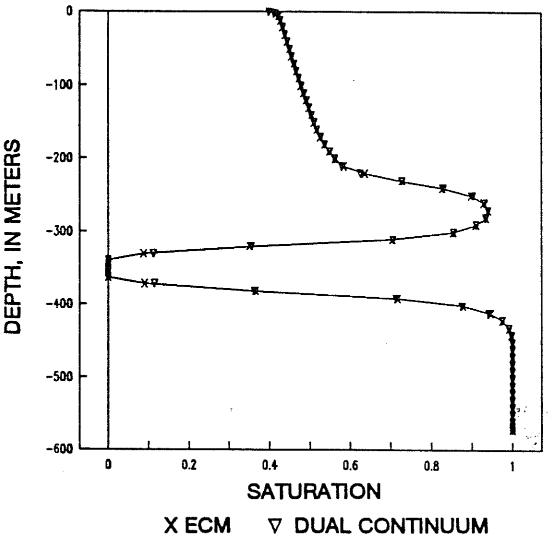

Figure 3. Comparison of the saturation versus depth profiles at 500 years following waste emplacement for the ECM and dual-continuum models.

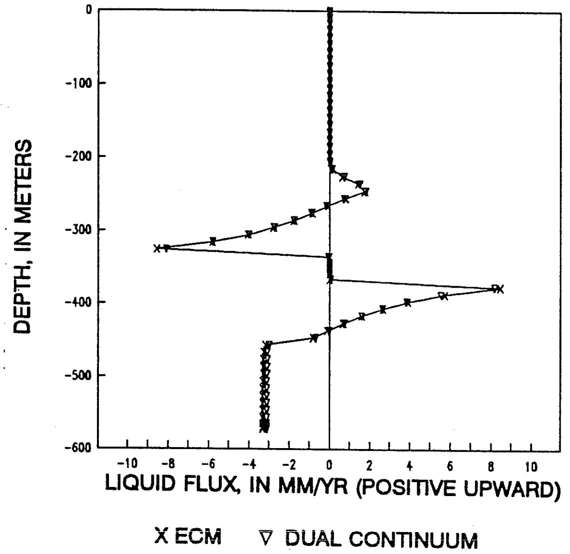

Figure 4. Comparison of the liquid flux versus depth profiles at 500 years following waste emplacement for the ECM and dual-continuum models.

remain in disequilibrium with the fracture continuum.

A modeling issue that has had potentially large influence on the rate of fluid exchange between the fracture and matrix continua is the definition of hydraulic properties of the fracture in a direction perpendicular to the fracture plane. It has been suggested (Wang and Narasimhan, 1985) that the appropriate relative permeability in this direction is the fractional wetted area, that is, the fraction of the fracture plane that is water-filled. The assumption of water potential equilibrium between fractures and the 0.5 mm of adjacent matrix allows these conceptual difficulties to be sidestepped. The fracture continuum contains matrix material immediately adjacent to the fractures and water must pass through this adjacent material to get from the fractures to the matrix continuum. Therefore, to remain internally consistent, the most appropriate fracture continuum properties to use in modeling its interaction with the matrix continuum are the welded tuff matrix intrinsic and relative permeabilities.

Heat generation curves for 8-year old spent nuclear fuel taken from Tsang and Pruess (1987) were used to represent the thermal loads caused by radioactive decay of the waste. Thermal properties for the Topopah Springs unit were also taken from the work by Tsang and Pruess (1987). An initial thermal loading of 114 kw/acre was assumed.

The ECM and dual-porosity models were compared for times ranging from 100 to 5000 years, which encompassed periods during which the dry-out zone was rapidly expanding and during which time the boiling isotherm had collapsed. Over this range of times, the results obtained by the ECM and dual-porosity methods for temperature, gas and capillary pressure, saturation, and vapor and liquid water fluxes were nearly identical. Figure 3 shows the bulk-rock saturation profiles at 500 years and figure 4 shows the liquid water fluxes for the same time. Both models predict complete dryout for several tens of meters above and below the repository located at about a 350m depth (figure 3). Superposition of the temperature profile at 500 years on these figures would show that vapor is condensing near the 100 °C isotherms at depths of approximately 250 and 450m. Figure 4 shows that water moves upward and downward away from these condensation zones located both above and below the repository. Maximum liquid fluxes of about 8 to 9 mm/yr are flowing back toward the repository. Downward drainage to the water table is about 3.4mm/yr at this time. The dual porosity model allows the component of the flux carried by the fracture continuum to be identified explicitly (figure 5). Surprisingly, due to the strong capillary pressure gradients, nearly all of the water refluxing back toward the repository is being carried by the matrix. This occurred even at 100 years when the maximum rate of refluxing toward the repository was between 25 and 30 mm/yr. Figure 5 also shows that, below the repository, an

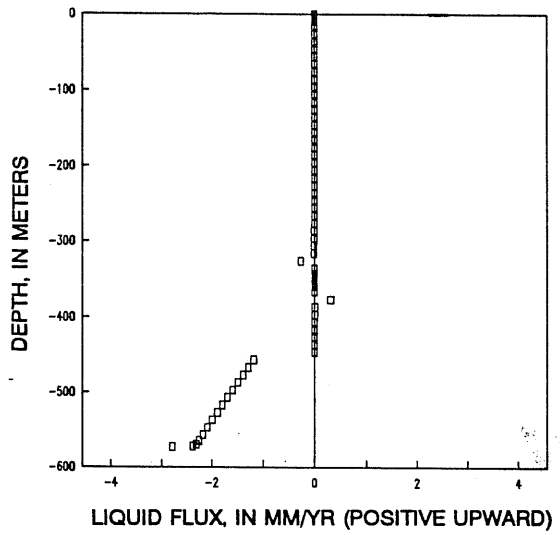

Figure 5. Liquid water flux versus depth for the fracture continuum at 500 years following waste emplacement, as calculated by the dual continuum model.

increasing amount of drainage is occurring through the fracture network as a result of the weak capillary pressure near the water table.

While the accuracy of the effective continuum model will degenerate eventually for decreasing matrix permeabilities and larger fracture spacings, this comparison showed it performed surprisingly well for fracture spacings and matrix permeabilities thought to be representative of the Topopah Spring unit. It should be kept in mind, however, that even the dual continuum approach represents only the average behavior of the fracture network. The absence of heterogeneity in fracture, as well as matrix properties, may underestimate the degree to which flow might become focussed in specific fractures or faults. Additionally, the effective permeability assumed for the fracture continuum was on the order of 10^{-15} m^2, which is approximately two orders of magnitude smaller than what has recently been measured for the Topopah Spring unit (LeCain and Walker, 1994).

Transient Water and Particle Movement Beneath an Alluvial Wash

The purpose of this study was to analyze the movement of water in the upper 120m beneath Pagany Wash, located on the eastern slope of Yucca Mountain, and thereby gain insight into the possible behavior of several similar washes that exist at the site. More specifically, the objectives of the numerical model were to (1) interpret the observed saturation, water potential and isotope data to infer the magnitude and direction of past and present-day water movement, (2) investigate the system dynamics, including identification of the controlling processes and features, and (3) develop an understanding of how the hydrologic system might respond to possible future climates.

Available data included porosity, saturation, water potential, stratigraphic and isotope (^3H, ^{14}C) data from two approximately 110m deep boreholes: UE-25 UZ#4, located in the center of the alluvial wash, and UE-25 UZ#5, located on a bedrock sideslope 38m to the southwest of UZ#4. To account for the heterogeneity reflected in the porosity profiles, each 1-m depth interval in the upper 120m at each hole was assigned to one of twelve porosity classes ranging from 0.05 to 0.60. The properties of each class were determined from correlations derived from a pre-existing data set between hydraulic conductivity, parameters that characterize the unsaturated moisture characteristic and hydraulic conductivity functions, and porosity (Kwicklis et al., 1993). Densely to moderately welded tuffs were assigned to the 0.05 to 0.30 porosity classes and given fracture porosity and permeability. However, based on their estimated capillary and hydraulic characteristics, the fractures were relatively nontrasmissive to water at water-potentials less than -1m.

The simulation domain extended 250m in a lateral direction, and 472m in depth to take advantage of known boundary conditions at the water table. The wash, conceptually located along the upper boundary within the central 10m, was assigned an infiltration rate of 20mm/yr, and the adjacent bedrock outcrop was assigned 0.1mm/yr. Initial conditions resulted from a uniform steady flow rate of 0.1 mm/yr throughout the entire domain. These boundary and initial conditions were suggested by 1-d simulations which determined that large fluxes were required to reproduce the observed saturation and water potentials profiles in the upper part of the boreholes, and conversely, the lower parts of the profiles were consistent with much smaller fluxes. Results are shown for the upper 120m, or elevations from 352 to 472m above the water table.

Many of the trends as well as values of the observed saturation and water potential profiles were reproduced by the numerical model, although some discrepencies remain due to uncertainties in hydrologic properties, assumptions concerning fracture-matrix potential equilibrium, and the

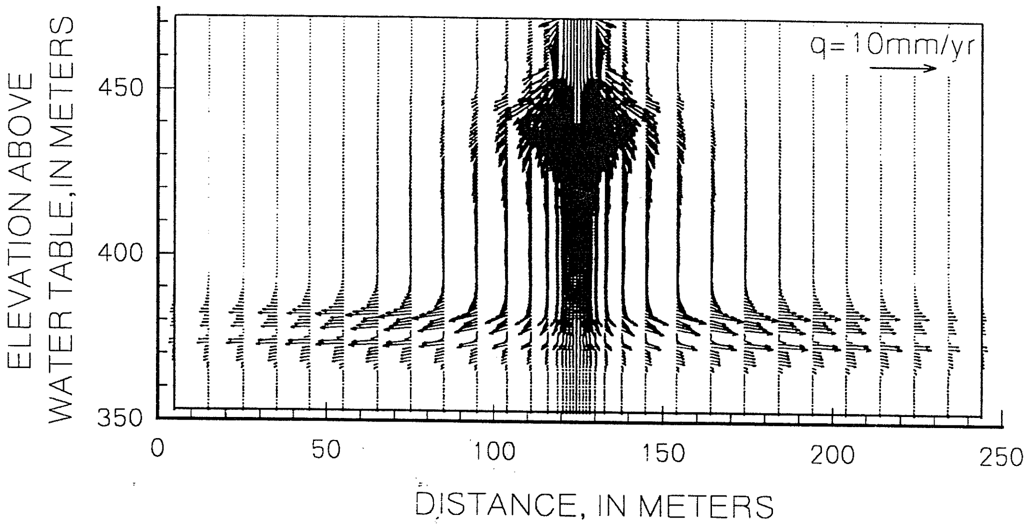

Figure 6. Water flux distribution beneath the wash at 10,000 years after the onset of increased flux in the wash.

conceptual model of infiltration. Additionally, the model results indicate the relative importance of various stratigraphic layers in promoting lateral spreading of focussed infiltration, thereby decreasing fluxes from peak values (figure 6). One such zone occurs in the nonwelded, relatively unfractured base of the Tiva Canyon Member between elevations of 430 to 450m (depths of 25 to 40m), where, due to a relatively abrupt change in degree of welding, porosity increases from 0.1 to 0.5, fractures terminate, and flow beneath the wash makes a transition from fracture to matrix dominated. A second significant interval in which lateral flow occurs is just above a low porosity vitrophyre at an approximately 360m elevation (110m depth). Lateral flow above this interval occurs partially in response to capillary barrier effects which occur at the interface between the rock pores of the nonwelded tuffs and the relatively larger openings of the fractures in the underlying densely welded tuffs. Water accumulates above this interface until it becomes sufficiently wet that fractures accept the water being delivered by the overlying rock matrix. As this water accumulates beneath the wash, it also flows laterally due to water potential gradients. Oldenburg and Pruess (1993) discuss modeling issues relevant the to investigation of capillary barriers with integrated finite difference codes such as TOUGH and TOUGH2..

A plot of steady-state vertical fluxes as a function of depth for the left half of the flow system (figure 7) shows that, by a 40m depth, peak fluxes beneath the wash have decreased to less than 5mm/yr, and that, at a 110m depth, fluxes are uniform and less than 1mm/yr. Thus, at least in the absence of faults, these layered sequences are predicted to play a key role in decreasing the amplitude of peak surface fluxes, and in delaying the arrival of surface derived moisture at the repository horizon.

To help assess the implications of the isotope data, the semianalytical particle tracking method developed by Lu (1994) was employed as a post processor to calculate particle movement under unsteady flow conditions. Velocities output from TOUGH for various elapsed simulation times were reformatted and used as input to the particle tracker, which traced particles applied along the upper boundary. The positions of those particles at various times after their release at t=1000yrs define the isochrons of figure 8. At an approximately 100m

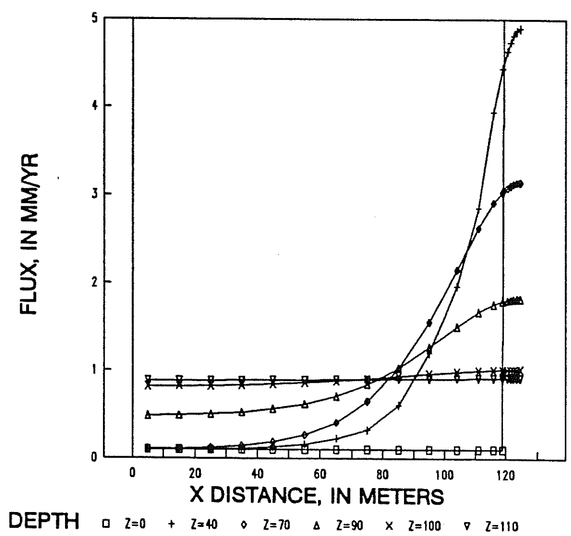

Figure 7. Steady-state vertical components of water flux across planes located at various depths beneath the wash.

depth in UZ#4, the model predicted a travel time of about 2,700 years, compared with the 1,000 year age date based on ^{14}C. At UZ#5, an age of approximately 5,100 years was predicted, compared with an age of 4900 years based on ^{14}C. The trend from younger water beneath the wash to older water with increasing distance from the wash, indicated by both the model results and the ^{14}C data, provide support for the argument that over millennia-long time scales, Pagany Wash has been an important source of recharge, despite evidence that that it has not been an important contributor over the last decade or longer (Hevesi and Flint, 1993). However, at locations where bomb-pulse ^{3}H has been found, the model predicts significantly longer advective travel times. Overprediction of travel times may have resulted because, in contrast to the model assumptions, much of the pore space in the densely welded tuffs in the Tiva Canyon Member is inaccessible to infiltrating water, which probably flows episodically but at high rates through near-surface fractures.

Since this application, TOUGH2 has been modified to output the x-, y- and z-components of liquid and gas fluxes and pore velocities, thereby greatly facilitating the application of particle tracking codes as post processors. That version of TOUGH2 requires, as user-supplied input, the x, y and z coordinate of the nodes associated with each cell. Fluid fluxes crossing the cell interfaces are resolved into their x-, y-, and z-components based on the coordinate information and the sign and magnitude of the flux, and assigned to the nodal points of the cell from which the flow is originating. Three-dimensional, nonorthogonal meshes are permitted, as long as standard integrated-finite difference assumptions have been adhered to in the mesh design.

SUMMARY

This paper describes three very different applications of the TOUGH code to hydrologic problems associated with the characterization of Yucca Mountain as a potential repository site. These included: (1) an investigation of steady water movement through a variably-saturated fracture network which suggested that flow path locations in natural systems may be quite dynamic and climate sensitive; (2) a dual continuum model of the hydrologic effects of waste-generated heat which supported the continued use of simpler, more computationally efficient effective continuum models in these types of analyses; and (3) an investigation of transient water and particle movement beneath an alluvial wash, which illustrated that contrasts in hydrologic properties of tuffs overlying the potential repository horizon could result in the formation of capillary barriers that would significantly decrease the amplitude of peak surface fluxes and delay the arrival of surface-derived moisture at the potential repository horizon.. Modeling issues and code modifications associated with these applications were discussed.

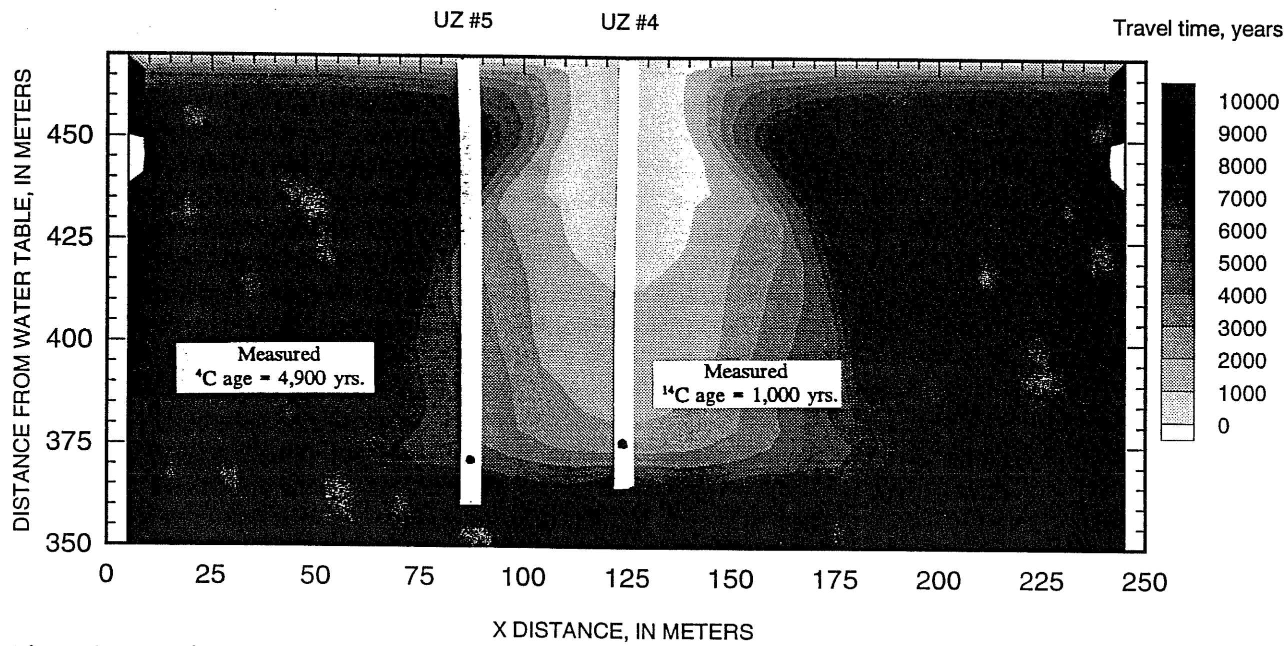

Figure 8. Travel time distribution of water particles released along the upper surface of the simulation region 1,000 years after the onset of increased flux in the wash.

REFERENCES

Buscheck, T.A., and J.J. Nitao, The analysis of repository-heat-driven hydrothermal flow at Yucca Mountain, in High-Level Radioactive Waste Management, Proceedings of the Fourth International Conference, Vol. 1, p. 847-867, American Nuclear Society, La Grange Park, Ill, 1993.

Hevesi, J.A., and A.L. Flint, The influence of seasonal climatic variability on shallow infiltration at Yucca Mountain, in High-Level Radioactive Waste Management, Proceedings of the Fourth International Conference, Vol. 1, p. 122-131, American Nuclear Society, La Grange Park, Ill, 1993.

Kwicklis, E.M., and R.W. Healy, Numerical investigation of steady liquid water flow in a variably saturated fracture network, Water Resources Research, vol. 29, no. 12, p. 4091-4102, 1993.

Kwicklis, E.M., A.L., Flint, and R.W. Healy, Estimation of unsaturated zone liquid water flux at boreholes UZ#4, UZ#5, UZ#7 and UZ#13, Yucca Mountain, Nevada, from saturation and water potential profiles, in Proceedings of the Topical Meeting on Site Characterization and Model Validation: Focus '93, p. 39-57, American Nuclear Society, La Grange Park, Ill., 1993.

LeCain, G.D., and J.N. Walker, Results of air-permeability testing in a vertical borehole at Yucca Mountain, Nevada, in High-Level Radioactive Waste Management, Proceedings of the Fourth International Conference, Vol. 4, p.2782-2788, American Nuclear Society, La Grange Park, Ill, 1994.

Lu, N., A semianalytical method of path line computation for transient finite-difference groundwater flow models, Water Resources Research, vol. 30, no. 8, p. 2449-2459, 1994.

Okusu, N.M., K. Karasaki, J.C.S. Long, and G.S. Bodvarsson, FMMG: A program for discretizing two-dimensional fracture/matrix systems, User's manual and listing, report, Lawrence Berkeley Lab., Berkeley, Calif., 1989.

Oldenburg, C.M., and K. Pruess, On numerical modeling of capillary barriers, Water Resources Research, vol., 29, no. 4, p. 1045-1056, 1993.

Pruess, K., and T.N. Narasimhan, A practical method for modeling fluid and heat flow in fractured porous media, Soc. Pet. Eng. J., 25(1), p. 14-26, 1985.

Pruess, K, J.S.Y. Wang, and Y.W. Tsang, On thermohydrologic conditions near high-level nuclear wastes emplaced in partially saturated fractured tuff: 1. Simulation studies with explicit consideration of fracture effects, Water Resources Research, vol. 26, no. 6., p. 1235-1248, 1990.

Pruess, K, J.S.Y. Wang, and Y.W. Tsang, On thermohydrologic conditions near high-level nuclear wastes emplaced in partially saturated fractured tuff: 2. Effective continuum approximation, Water Resources Research, vol. 26, no. 6., p. 1249-1261, 1990.

Tsang, Y.W., and K. Pruess, A study of thermally induced convection near a high-level nuclear waste repository in partially saturated fractured tuff, Water Resources Research., vol. 23, no. 10, 1958-1966, 1987.

Wang, J.S.Y. and T.N. Narasimhan, Hydrologic mechanisms governing fluid flow in a partially saturated, fractured, porous medium, Water Resources Research, vol. 21, no.12, p. 1861-1874, 1985.